Journal of Sound and Vibration (2002) **258**(4), 633–648
doi:10.1006/jsvi.2002.5142, available online at http://www.idealibrary.com on IDEAL®

ANALYSIS OF WAVELETS IN CHAOTIC STATES FOR A ONE-DEGREE-OF-FREEDOM SYSTEM WITH VISCOELASTIC RESTRAINTS

W. GLABISZ

Institute of Civil Engineering, Wroclaw University of Technology, Wyb. Wyspianskiego 27, 50-370 *Wroclaw, Poland. E-mail: glabisz@i14odt.iil.pwr.wroc.pl*

(*Received* 27 *November* 2000, *and in final form* 9 *October* 2001)

A qualitative numerical technique is presented for identifying chaotic states of a non-linear one-sided constrained one-degree of freedom (1-d.o.f.) deterministic system under a dynamic non-conservative load. Discrete wavelet analysis in its classic and packet versions was used to search for the boundaries of chaotic and non-chaotic solutions. The results obtained were verified by an analysis of the Lyapunov exponents of the investigated system. On the basis of numerical tests, one can state that wavelet analysis may be a fast and reliable tool suitable for searching for the boundaries of chaotic and non-chaotic solutions.

1. INTRODUCTION

The search for accurate ways of describing real phenomena leads inevitably to non-linear models. A mathematical description of the behaviour of such models, based on non-linear mechanics is usually in the form of complex systems of partial differential equations. Chaos is one of the phenomena based on a non-linear description [1–5]. The (numerical) analysis of chaotic phenomena is one of the basic ways of investigating critical states of non-linear models. The chaotic state of a system may be indicated by, for example, phase portraits, time-history response, Fourier analysis, Poincaré maps, auto-correlation analysis or bifurcation diagrams, but its existence is proved conclusively by a laborious, time-consuming quantitative analysis of the system's Lyapunov exponents [1–5].

One of the tools by which the characteristic features of a system's chaotic states can be identified is wavelet analysis of the system's responses [6–11]. Because of the nature of the base functions employed, this analysis is particularly suitable for the description of non-stationary states and so can be an alternative to the above-mentioned qualitative identification techniques.

The aim of this paper is to demonstrate the effectiveness of the discrete wavelet analysis and packet wavelet analysis of a system's response, ensuring fast qualitative identification of the system's chaotic states. This is done, using as an example, a non-linear analysis of a system with one degree of freedom (1 d.o.f.) and one-sided viscoelastic constraints. The 1-d.o.f. system considered could be a model of the behaviour of dynamically loaded cantilever structural elements with limited displacements and varying constraints.

Wavelet analysis is applied to many engineering problems such as the analysis of different (mainly non-stationary) signals [12–17], the diagnosis of damage and cracks [18–21], and the identification of design parameters [22–24] and the identification of damping [25–28].

0022-460X/02/$35.00

Until now wavelet analysis has seldom been used to analyze chaotic systems. It was used to detect small-amplitude harmonic components in motions considered as chaotic [29]. A continuous wavelet transform was used in the analysis of the statistical measures of wavelet expansion coefficients in the Ueda variant of the Duffing oscillator [30] and a harmonic wavelet transform and a Poincaré map were used to identify the type of motions in a non-linear dynamical system [31]. A continuous wavelet transform was used in the analysis of a non-linear system in the vicinity of its Hopf bifurcation point [32] and the so-called cross-wavelet analysis was applied to the Duffing oscillator [33].

In the present paper, a short introduction to wavelet and wavelet packet analysis is given, an equation of the geometrically and physically non-linear motion of a dynamically loaded 1-d.o.f. system with one-sided constraints is formulated and several numerical analyses showing the effectiveness of the proposed qualitative approach to the identification of its chaotic states are presented.

2. SHORT INTRODUCTION TO WAVELET AND WAVELET PACKET ANALYSIS OF A SIGNAL

Wavelets $\psi(t)$, as the name suggests, are "small waves" having a limited range and oscillatory character. Wavelets make up particular sets of base functions in a description of discrete and irregular functions (signals) found in the response of real physical systems, especially in chaotic systems. In contrast to Fourier bases, whose elements are simple trigonometric functions with an infinite support, wavelets with their limited range and generally fast disappearance make up bases located well in frequency and time t. Wavelet function bases are formed by scaling (using parameter a) and shifting in time (using parameter b) an initial wavelet (mother wavelet) $\psi(at+b)$, leading to the so-called scalable, hierarchical representation of a considered function or signal. As with discrete Fourier and discrete short-time Fourier transforms, one has, for $a=2^{-j}$ and $b=k2^{-j}$ where $k,s\in Z$, the discrete wavelet transform.

One can consider a signal to consist of a smooth part $(f_j(t))$, constituting the core of the description, and a part $(d_j(t))$ containing information about the (usually small) fluctuations of the signal. The distinction between the smooth part and the fluctuations is determined by the resolution, that is, by the scale below which the fluctuation of a signal cannot be discerned. The resolution level is labelled by an integer j. A more accurate description of a signal (a description at a higher resolution, $j+1$, i.e., $f_{j+1}(t)$) can be obtained if fluctuations $d_j(t)$ (which a scale defined as 2^{-j} permits to be perceived) are added to its lower-resolution; $j, f_j(t)$ description [8]. This can be represented as

$$f_{j+1}(t)=f_j(t)+d_j(t). \tag{1}$$

By reducing the scale, an increasingly more accurate description of the analyzed signal is obtained as

$$f(t)=f_j(t)+\sum_{k=j}^{\infty} d_k(t). \tag{2}$$

This approach to the description of the function spaces of square-integratable functions $(f(t)\in L^2(R))$ can be interpreted as a search for a description of them in space $(V_j(f(t)\in V_j)$, supplemented with the details of the description in spaces $\{W_k\}$ $(d_j(t)\in W_j)$. Spaces V_j and W_j are mutually orthogonal $(W_j\perp V_j)$. The so-called scaling function, $\phi(t)$ and the functions resulting from its shifts k form the basis $\{\phi_{jk}(t)\}$ of space

V_j, where $\phi_{jk} = 2^{j/2}\phi(2^j t - k)$. As is known, $V_0 \subset V_1$ and so each function in V_0 can be represented by a base of space V_1. In particular, scaling function $\phi(t) \in V_0$ can be expressed in the basis $\{\phi_{1k}(t)\}$ as

$$\phi(t) = \sum_k h_k \phi_{1k}(t) = \sqrt{2} \sum_k h_k \phi(2t - k). \tag{3}$$

Equation (3) is called a dilation equation and set of expansion coefficients $\{h_k\}$ is referred to as a low-pass filter.

Space W_0 constitutes an orthogonal supplement to space V_0 (sometimes referred to as a central space) which as a result becomes space V_1 thus,

$$V_1 = V_0 \oplus W_0 \tag{4}$$

and so since wavelet $\psi(t - k) \in W_0$ and $V_0 \subset V_1$, one can represent $\psi(t)$ as a superposition of the basis functions in space V_1 by

$$\psi(t) = \sum_k g_k \phi_{1k}(t) = \sqrt{2} \sum_k g_k \phi(2t - k), \tag{5}$$

where the set of coefficients $\{g_k\}$ is called a high-pass filter. Equation (5) is called a wavelet equation. The scaled versions of function $\psi(t)$ constitute the basis of space $W_j : \{\psi_{jk}(t) = 2^{j/2}\psi(2^j t - k)\}$. Equations (3) and (5) are referred to as two-scale relations. The discrete wavelet transform of $f(t)$ can be shown as the decomposition

$$f(t) = \sum_k f_k^j \phi_{jk}(t) + \sum_{l=j}^{\infty} \sum_k d_k^l \psi_{lk}(t), \tag{6}$$

where $f_k^j = \langle \phi_{jk}, f \rangle$ and $d_k^j = \langle \psi_{jk}, f \rangle$. For the scale parameter in the form $a = 2^{-j}$, the hierarchical wavelet decomposition (6) produces signal components whose spectra form the so-called consecutive octave bands.

In certain applications, for example in chaotic states, analysis, the wavelet decomposition may not be fine enough to meet the problem requirements. To solve this, one uses continuous wavelet transformation substituting a smaller increment for the scale parameter a or by applying wavelet packets.

A wavelet packet is a generalization of a wavelet in that each octave frequency band of the wavelet spectrum is further subdivided into finer frequency bands by using the two-scale relations repeatedly. The space V can be decomposed into a direct sum of two orthogonal subspaces defined by their basis functions given by equations (3) and (5). This splitting algorithm can be used to decompose W spaces as well. For example, if one defines

$$w_2(t) = \sqrt{2} \sum_k h_k \psi(2t - k), \quad w_3(t) = \sqrt{2} \sum_k g_k \psi(2t - k), \tag{7}$$

then $\{w_2(t - k)\}$ and $\{w_3(t - k)\}$ are orthonormal basis functions for the two subspaces whose direct sum is W_1.

In general, for $n = 0, 1, \ldots$ one defines a sequence of functions

$$w_{2n}(t) = \sqrt{2} \sum_k h_k w_n(2t - k), \quad w_{2n+1}(t) = \sqrt{2} \sum_k g_k w_n(2t - k). \tag{8}$$

So far, using the combination of $\{\phi(2^j t - k)\}$ and $\{\psi(2^j t - k)\}$ has been used to form a basis for V_J, and now one has a whole sequence of $w_n(t)$ at one's disposal. Various combinations of these and their dilations and translations can give rise to various bases for the function space. One has a whole collection of orthonormal bases generated from

$\{w_n(t)\}$ called a "library of wavelet packet bases". The function of the form $w_{njk} = 2^{j/2} w_n(2^j t - k)$ is called a wavelet packet.

3. PROBLEM FORMULATION

Let one consider the vibration of a 1-d.o.f. system consisting of an elastically fixed, infinitely rigid massless bar of length l, with a concentrated mass m whose position on the bar is given by co-ordinate x (Figure 1). The system is assumed to be loaded with a non-conservative dynamic force $P(t)$ which acts in the direction specified by the follower parameter $\alpha(t)$. Bar rotation $q(t)$, which is the deflection of the bar from its vertical form, was assumed as the problem's generalized co-ordinate. The non-stress form of the deflected bar is defined by imperfection q_0. The rigidity of the elastic fixation of the bar is defined by time-variable function $k(t)$ and its viscous damping, by function $c(t)$. The motion of the system is additionally limited by two elastic-damping one-sided constraints whose rigidity, viscous damping and vertical and horizontal position are specified respectively by functions $(k_l(t), c_l(t), h_l(t), \Delta_l(t))$ for the left-side spring (l) and $(k_r(t), c_r(t), h_r(t), \Delta_r(t))$ for the right-side spring (r). If one considers the condition of the system's dynamic equilibrium as a zero sum of the moments of all the forces (including the inertia forces) relative to the point of fixation of the bar and introduce non-dimensional quantities $\xi = x/l, \xi_l = h_l/l, \xi_r = h_r/l$, $\xi_{\Delta l} = \Delta_l/l$ and $\xi_{\Delta r} = \Delta_r/l$ specifying the position of mass m and that of the left and right constraints, one easily deduces (assuming that the problem is geometrically linear, i.e., $q(t) \to 0$) the equation of the

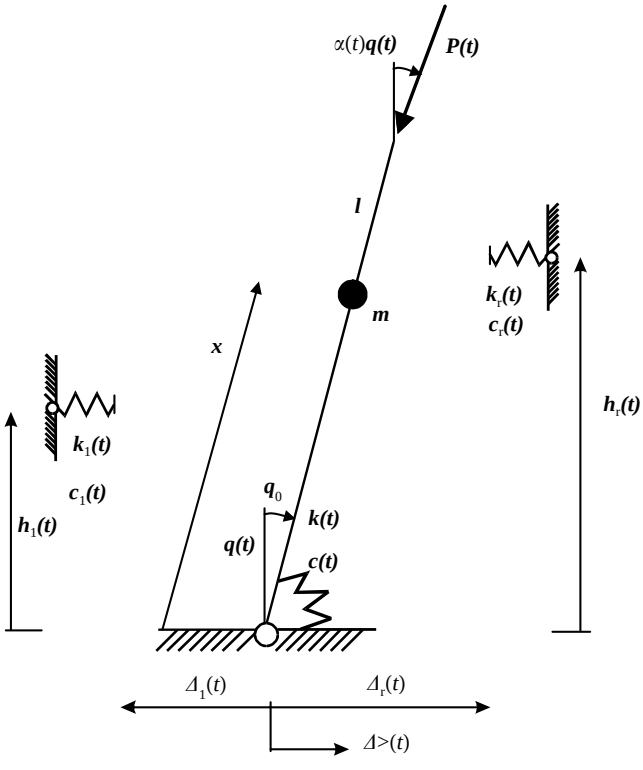

Figure 1. Diagram of analyzed model.

system's motion as

$$m(\xi l)^2\ddot{\boldsymbol{q}}(t) + c(t)\dot{\boldsymbol{q}}(t) + c_r(t)(\xi_r l)\mathrm{H}[q(t)(\xi_r l) - \xi_{\Delta r} l]\dot{\boldsymbol{q}}(t)(\xi_r l) + c_l(t)(\xi l)\mathrm{H}[\xi_{\Delta l} l - q(t)(\xi_l l)]\dot{\boldsymbol{q}}(t)(\xi_l l) + k(t)[q(t) - q_0(t)] + k_r(t)(\xi_r l)\mathrm{H}[q(t)(\xi_r l) - \xi_{\Delta r} l][q(t)(\xi_r l) - \xi_{\Delta r} l] + k_l(t)(\xi_l l)\mathrm{H}[\xi_{\Delta l} l - q(t)(\xi_l l)][q(t)(\xi_l l) - \xi_{\Delta r} l] = P(t)q(t)l\eta(t), \tag{9}$$

where $\eta(t) = [1 - \alpha(t)]$ and differentiation with respect to time t is denoted by dots, and $H(\cdot)$ denotes the Heaviside function.

If the finite rotations $q(t)$ are allowed, the equation of the geometrically non-linear problem assumes the form

$$m(\xi l)^2\ddot{\boldsymbol{q}}(t) + c(t)\dot{\boldsymbol{q}}(t) + c_r(t)(\xi_r l)\mathrm{H}[tg\, q(t)(\xi_r l) - \xi_{\Delta r} l]\frac{1}{\cos^2 q(t)}\dot{\boldsymbol{q}}(t)(\xi_r l) + c_l(t)(\xi_l l)\mathrm{H}[\xi_{\Delta l} l - tg\, q(t)(\xi_l l)]\frac{1}{\cos^2 q(t)}\dot{\boldsymbol{q}}(t)(\xi_l l) + k(t)[q(t) - q_0(t)] + k_r(t)(\xi_r l)\mathrm{H}[tg\, q(t)(\xi_r l) - \xi_{\Delta r} l][tg\, q(t)(\xi_r l) - \xi_{\Delta r} l] + k_l(t)(\xi_l l)\mathrm{H}[\xi_{\Delta l} l - tg\, q(t)(\xi_l l)][tg\, q(t)(\xi_l l) - \xi_{\Delta l} l] = P(t)l\sin[q(t)l\eta(t)]. \tag{10}$$

The one-sided constraints and arbitrary forms of the system's rigidity functions cause both equations (9) and (10) to describe physically non-linear problems.

4. NUMERICAL ANALYSIS

For a certain choice of parameters the investigated system, whether its behaviour may or may not be described by equation (9) or (10), behaves chaotically, which can be established unequivocally (quantitatively) by an analysis of its Lyapunov exponents. Using as an example, a system loaded with a dynamic non-conservative force, an analysis of its Lyapunov exponents for some follower parameters α will be made. Ranges of the variability of parameter α at which the system enters chaotic states will be determined and the system's responses for these parameters will be subjected to wavelet analysis. Equation (10) and the equations resulting from the linearization of it make up a mathematical model of the system's behaviour. At $q(t) \to 0$ the linearization generates a system description represented by equation (9).

In the considered cases it is assumed that $m = l = \xi = 1,\ q_0 = 0,\ c = c_r = c_l = 0{\cdot}01,\ k = 10,\ k_r = k_l = 1000,\ \xi_l = \xi_r = 0{\cdot}5,\ \Delta_r = -\Delta_l = 0{\cdot}1,\ P(t) = 5\sin(3t)$ and the initial deflection and velocity are $q(0) = 0{\cdot}1$and $\dot{\boldsymbol{q}}(0) = 0{\cdot}0$ respectively. Analyzing (in a discrete set of points) the effect of follower parameter α in the range $\alpha \in (-0{\cdot}5; 2{\cdot}5)$, it is obvious that at $\alpha \leqslant 0{\cdot}0$ and $\alpha \geqslant 2{\cdot}0$ one of the Lyapunov exponents is positive, which means that the system is chaotic. A systematic search for the limits of the chaotic solutions shows that the boundary close to zero is in the interval $\alpha \in (0{\cdot}00; 0{\cdot}02)$ and the boundary close to $\alpha = 2{\cdot}0$ is in the interval $\alpha \in (1{\cdot}98; 1{\cdot}99)$. The convergence diagrams for the Lyapunov exponents in the vicinity of $\alpha = 0{\cdot}0$ and $2{\cdot}0$ are shown, respectively, in Figures 2 and 3, where exponent values and the number of analysis time steps are shown on the Y- and X-axes, respectively. The time step is $\Delta t = 0{\cdot}025$ s. An analysis of the convergence of the Lyapunov exponents for double the time confirmed the results shown in Figures 2 and 3. The test proposed in reference is [1] used for estimating the relative/absolute convergence of the Lyapunov exponents algorithms presented in references [34,35]. The oscillatory character of the convergence plot of the Lyapunov spectrum is typical for some attractors [36–38].

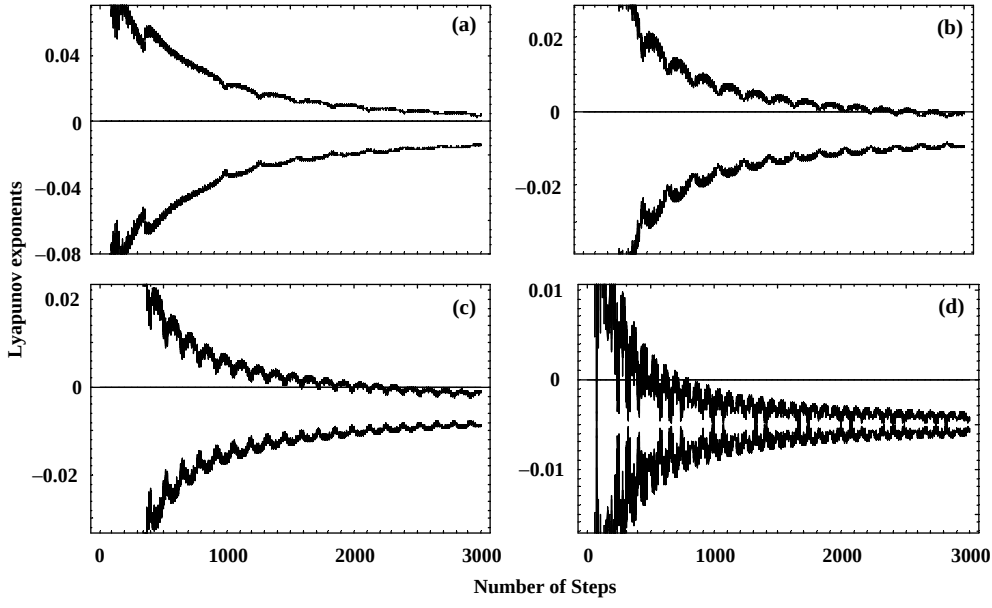

Figure 2. Convergence plot of Lyapunov exponents at (a) $\alpha = 0{\cdot}0$, (b) $\alpha = 0{\cdot}02$, (c) $\alpha = 0{\cdot}04$, and (d) $\alpha = 0{\cdot}1$.

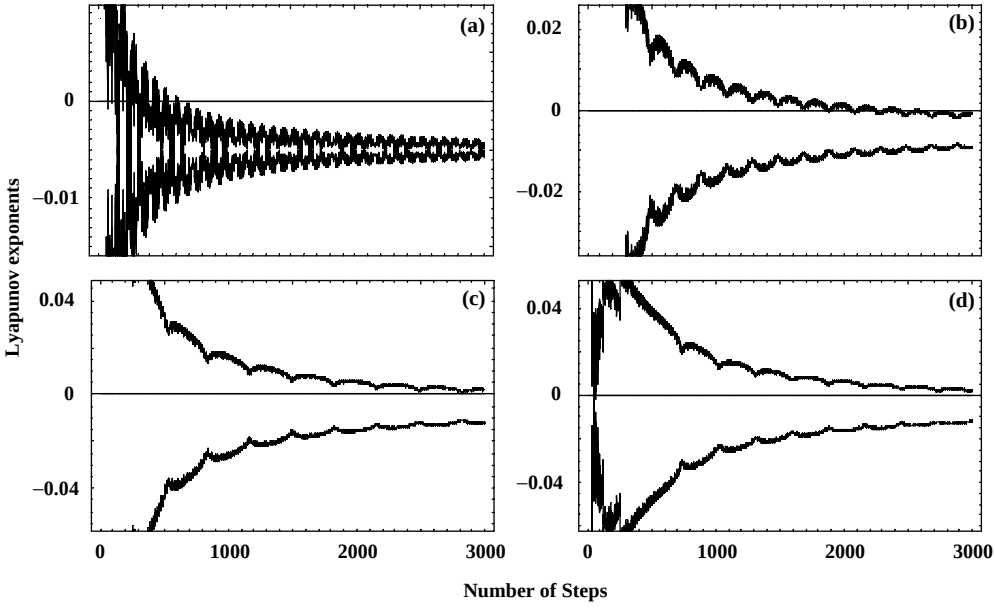

Figure 3. Convergence plot of Lyapunov exponents at (a) $\alpha = 1{\cdot}9$, (b) $\alpha = 1{\cdot}98$, (c) $\alpha = 1{\cdot}99$ and (d) $\alpha = 2{\cdot}0$.

The wavelet analysis is based on the deterministic system's response (signal) in the form of a discrete set of displacements $q(t)$ of size 2^{14} of equally spaced N time samples taken in the first 2000 s of the system vibration. The adopted sampling rate corresponds to about 15 readings taken during the free vibration period of the investigated system. The values of

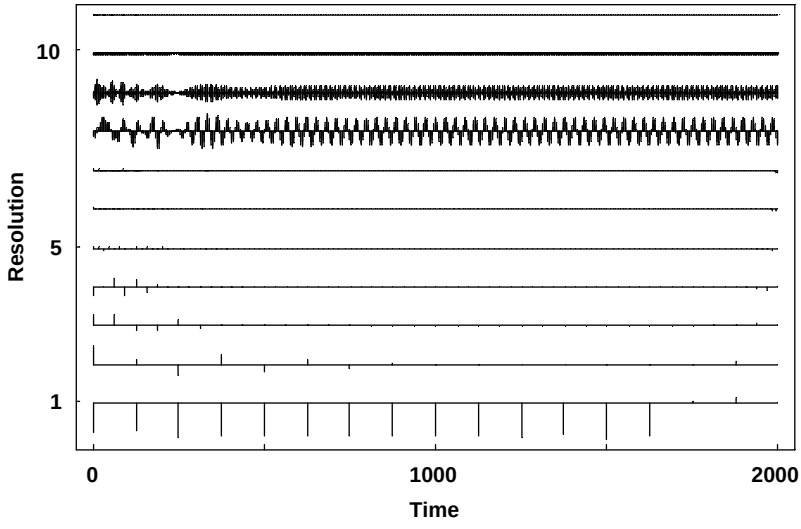

Figure 4. Chaotic signal ($\alpha = 0{\cdot}0$) wavelet expansion coefficients at different resolutions.

data points that are padded at the boundaries are determined by the choice of the periodic ($q_{i+N} = q_i$) boundary condition. The Daubechies wavelet of the order of 12 was used in the analysis of the signal [6]. Also other wavelets, i.e., the Shannon wavelet, the Mallat wavelet, and the Haar wavelet, were used to analyze the signal [6,8,9,11]. The results of all the analyses were found to be in agreement. In the case of the Haar wavelet, although the symptoms of a transition to chaos were on the whole preserved, the well-known weaknesses of the signal description based on this type of wavelet became apparent [6–9]. The time distributions of system response wavelet expansion coefficient values for a chaotic state ($\alpha = 0{\cdot}0$) and a non-chaotic state ($\alpha = 0{\cdot}1$) at the particular signal perception levels [8] are shown in Figures 4 and 5. The 11 sublists are plotted and stacked together. The lowest level plot ($j = 1$) is the residual trend (f_k^j); the topmost ($j = 11$), the finest details (d_k^j). The expansions are markedly different, particularly at higher resolutions, and thus easily distinguishable. The analyzed states are practically indistinguishable in the time domain as illustrated by fragments of the response of the system in the chaotic state ($\alpha = 0{\cdot}0$) (Figure 6(a)) and in the non-chaotic state ($\alpha = 0{\cdot}1$) (Figure 6(b)), which are almost identical except for the magnitude of amplitudes. In Figure 7 the differences in power spectrum analysis for chaotic states ($\alpha = 0{\cdot}0$ (see Figures 7(a) and 7(c) and $\alpha = -0{\cdot}05$ (Figure 7(e)) and non-chaotic states ($\alpha = 0{\cdot}1$ Figures 7(b) and 7(d), and $\alpha = 0{\cdot}15$ (Figure 7(f)) are shown. The existing qualitative differences in the power spectrum are not so sharp as the differences in the distribution of wavelet expansion coefficients for $\alpha = 0{\cdot}0$ (Figure 4) and $\alpha = 0{\cdot}1$ (Figure 5). For $\alpha = -0{\cdot}05$ (Figure 7(e)) and $\alpha = 0{\cdot}15$ (Figure 7(f)) these differences are evident and they permit to distinguish chaotic and non-chaotic states uniequivically.

The differences between chaotic and non-chaotic states can be seen even more clearly by applying wavelet packet signal analysis [6–8]. In wavelet decomposition one ignores the high-frequency part and keeps splitting the low-frequency part. In wavelet packet decomposition, one can also choose to split the high-frequency part into low- and high-frequency parts. So in general, wavelet packet decomposition divides the frequency space into various parts allowing better frequency localization of the signal. Wavelet packet analysis (up to six decompositions, resulting in 64 levels of resolution) is applied here to

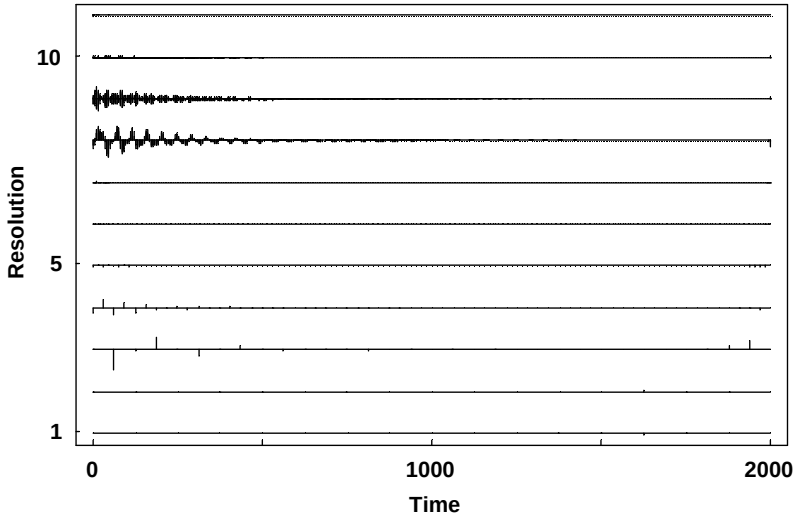

Figure 5. Non-chaotic signal ($\alpha = 0{\cdot}1$) wavelet expansion coefficients at different resolutions.

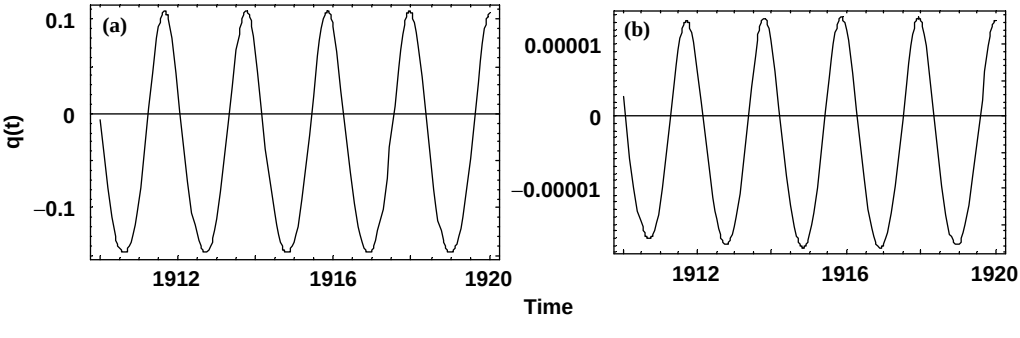

Figure 6. Fragments of the response of the system $q(t)$ at (a) $\alpha = 0{\cdot}0$ and (b) $\alpha = 0{\cdot}1$.

signals in the vicinity of the second of the previously determined boundaries between non-chaotic and chaotic states (Figure 3). Selected levels (identical for both states) of the wavelet packet decomposition (based on Daubechies filter of order 12) of the signals are shown in Figures 8 and 9. The shown resolution levels correspond to signal frequencies in the range 0·0 –0·25 Hz). There are marked differences in the distribution and magnitude of the wavelet expansion coefficients. Examples of significant differences between non-chaotic and chaotic signal wavelet packet analyses can also be easily found in other frequency ranges. The duration of the search for the boundaries of chaotic and non-chaotic solutions using wavelet analysis of the system's response was two orders less time consuming than the laborious analysis of its Lyapunov exponents.

If one defines the cumulative energy of the signal wavelet expansion as $\sum_{i=1}^{n} |c_i|^2$, where $|c_i| \geqslant |c_{i+1}|$ and normalizes this energy to 1, then an analysis of the number of coefficients that are significant from the energy point of view gives a representation of the character of a particular response. If one plots signal energy as a function of the number of included coefficients (ordered from the highest value in absolute value terms), then it becomes clear that chaotic states are characterized by a larger number of significant wavelet expansion

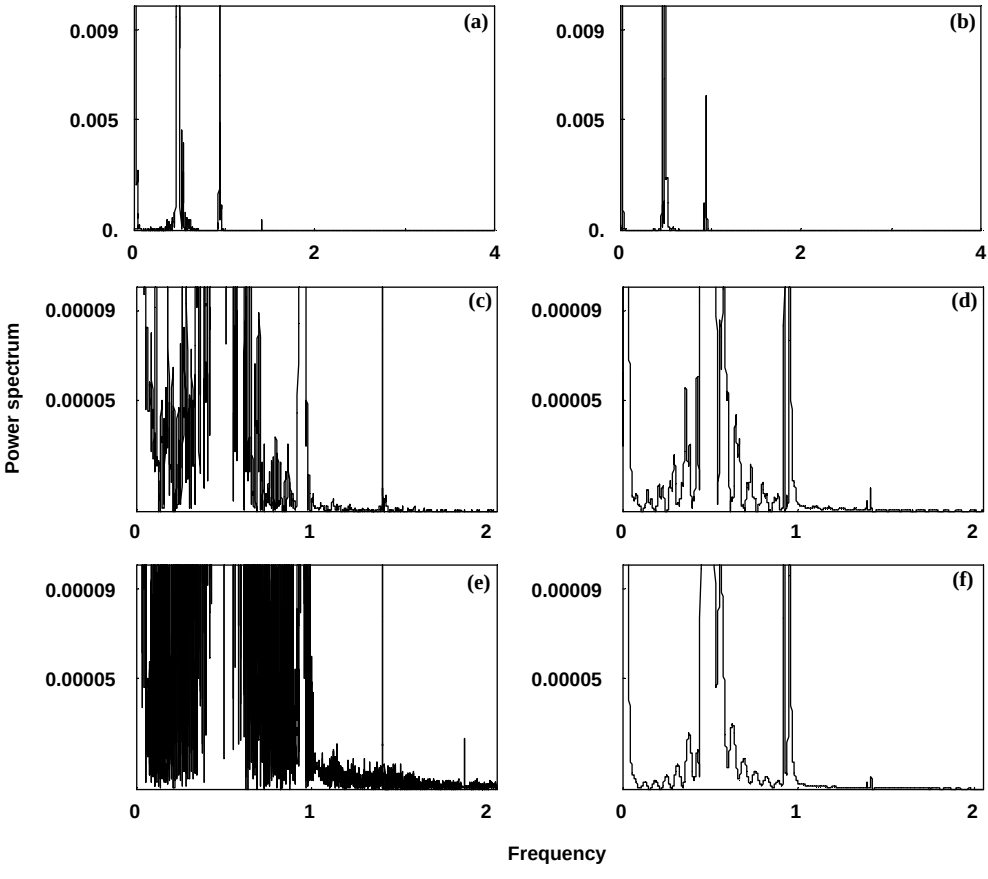

Figure 7. Power spectrum of a chaotic signal: (a), (c) $\alpha = 0{\cdot}0$; (e) $\alpha = -0{\cdot}05$; and a non-chaotic signal (b, d) $\alpha = 0{\cdot}1$; (f) $\alpha = 0{\cdot}15$.

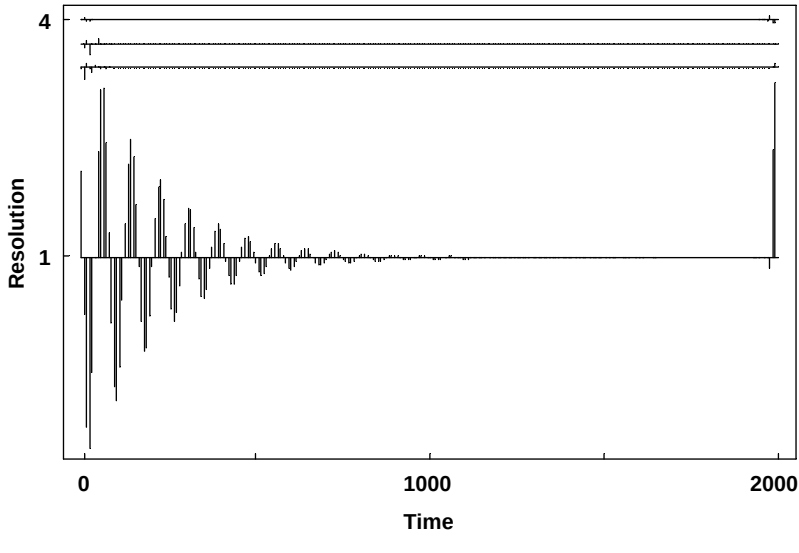

Figure 8. Non-chaotic signal ($\alpha = 1{\cdot}96$) wavelet coefficients at the lowest resolutions.

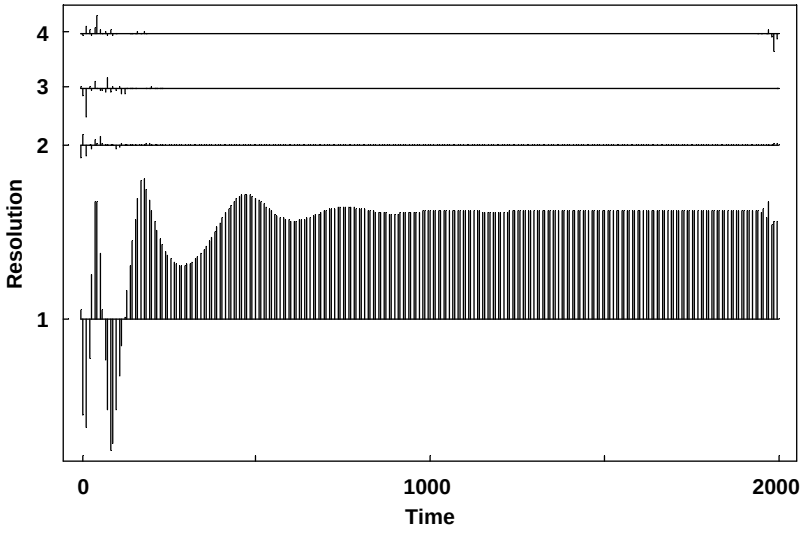

Figure 9. Chaotic signal ($\alpha = 2{\cdot}0$) wavelet coefficients at the lowest resolutions.

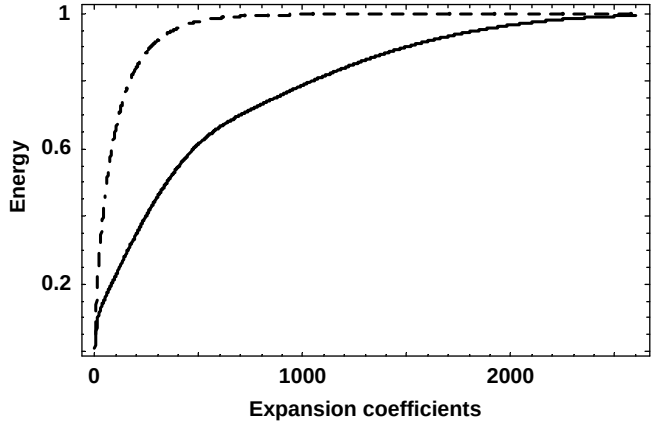

Figure 10. Non-chaotic ($\alpha = 1{\cdot}96$, dashed line) and chaotic ($\alpha = 2{\cdot}0$, solid line) signal energy versus number of wavelet coefficients.

coefficients. This means that in order to keep the same level of signal energy in chaotic states one must consider a significantly larger number of coefficients than the one for the same energy level in a non-chaotic state (Figure 10). The wavelets and the assumed boundary condition may cause local boundary disturbance in the wavelet coefficient distribution. This disturbance (appearing only in less than 10 from among 16 384 coefficients) insignificantly influences the energy distribution.

In wavelet packet transformations, one can choose not to decompose a particular subspace while decomposing others so that there may be choices for a signal representation. As is usual in such cases one needs to choose from among all the representations the one that represents the signal most efficiently. By ''efficient'' one means that a signal can be represented by a small number of wavelet packets. The basis for the decomposition is chosen such that the weight of the coefficients is concentrated on a small number of wavelet packets and a large number of coefficients are close to zero. The

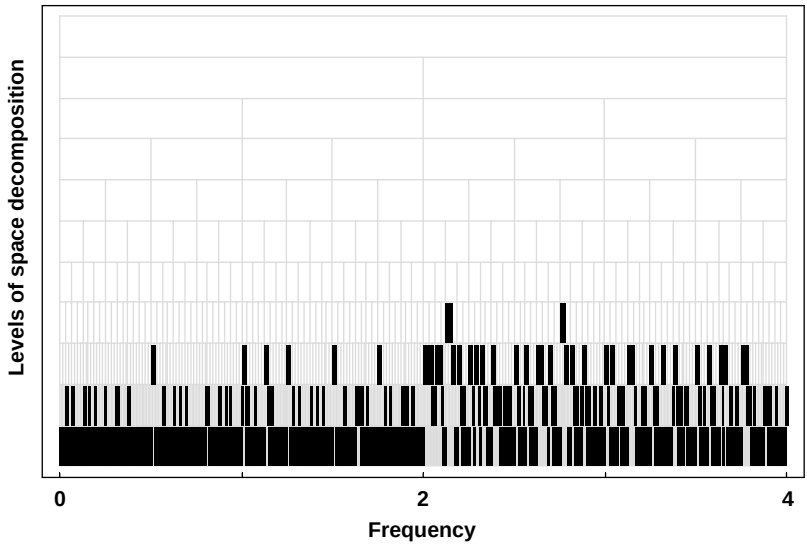

Figure 11. Position of the best basis for the non-chaotic state ($\alpha = 0{\cdot}1$).

criterion generally used for choosing the best basis for a given signal is the minimum entropy criterion [39]. For each set $\{v_i\}$of the decomposition coefficients of a signal for a particular choice of the wavelet packet basis, one associates a non-negative quantity $-\sum_i v_i^2/||v||^2 \log_2(v_i^2/||v||^2)$ called entropy, where $||v||^2 = \sum_i v_i^2$. Intuitively, the entropy defined above gives a measure of how many effective components are needed to represent the signal for a specific basis. The best basis is the one which produces the least entropy. One can visualize how the frequency space is split or equivalently what basis functions are chosen by plotting the best basis location. Figure 11 shows the location of the best basis for the non-chaotic signal ($\alpha = 0{\cdot}1$). The top row represents the original space. Each decomposition splits each frequency space in the previous level into two subspaces. The best basis is the combination of the basis functions from the shaded spaces. Figure 12 shows the location of the best basis for chaotic signal ($\alpha = 0{\cdot}0$). As a rule for chaotic signals the lowest row which corresponds to the lowest resolution level is chosen as the best basis location.

There is full agreement between the results obtained (for presently used parameters) from an analysis of the Lyapunov exponents of a geometrically linear system described by equation (9) and those obtained using equation (10). A wavelet analysis of the response of the system described by equation (9) preserves (similar to the above) the characteristic qualitative features of the transition from non-chaotic to chaotic states. The differences between the approach based on equation (9) and that based on equation (10) are visible at lower scales, which corresponds to the higher frequency fractions (higher resolution levels) of the signal components. The results of a wavelet packet analysis of signals that are responses of the system described respectively by equation (9) (Figure 13(a)) and equation (10) (Figure 13(b)) at $\alpha = 2{\cdot}0$ are shown in Figure 13. The figure shows a range in which differences occur—these are exclusively quantitative differences. The agreement between the approach based on a geometrically linear description (9) and the approach which permits finite displacements $q(t)$ (10) was obtained through the specific choice of problem parameters. If one assumes, for example, that $m = l = \xi = 1, q_0 = 0, c = c_r = c_l = 0{\cdot}01$, $k = 10, k_r = k_l = 1000, \xi_l = \xi_r = 0{\cdot}5, \quad \Delta_r = -\Delta_l = 0{\cdot}3, P(t) = sin(6t), \quad \alpha = 9{\cdot}0$ and the

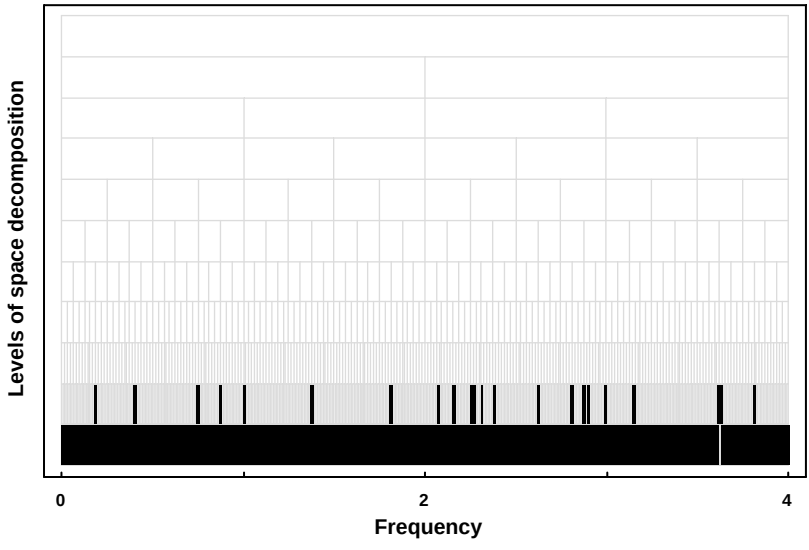

Figure 12. Position of the best basis for the chaotic state ($\alpha = 0{\cdot}0$).

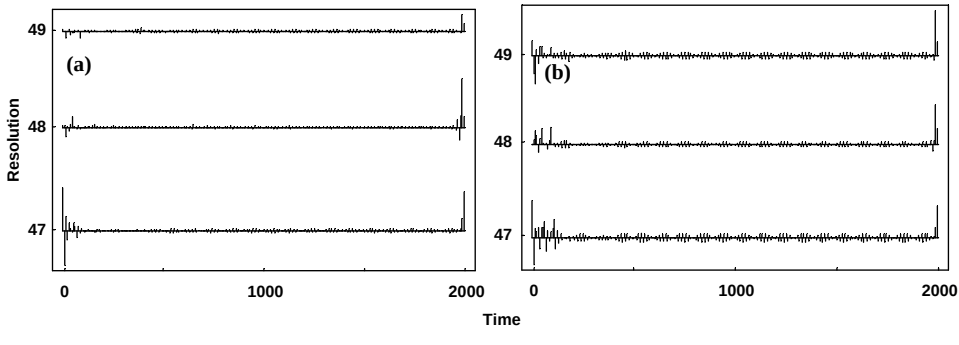

Figure 13. Selected resolution levels of chaotic signal ($\alpha = 2{\cdot}0$) wavelet coefficients for descriptions by (a) equation (9) and (b) equation (10).

initial deflection and velocity have values respectively $q(0) = 0{\cdot}1$and $\dot{q}(0) = 0{\cdot}0$, the character of the system response may be radically different, both qualitatively and quantitatively, depending on whether equation (9) or (10) is used. An analysis of the Lyapunov exponents for these parameters shows that if equation (9) representing the linear geometric approach is applied, the system appears to be chaotic (Figure 14(a)). According to an analysis of the Lyapunov exponents based on equation (10) representing the geometrically non-linear approach, the system does not exhibit any features of a chaotic system (Figure 14(b)).

Figures 15–17 show results of a wavelet packet analysis of signals that are responses of the system described respectively by equation (10) (Figure 15), linearized equation (10) with four terms of expansion $q(t)$ into a Taylor series (Figure 16) taken into account, and linearized equation (10) with two terms of the expansion (Figure 17) taken into account. The resolution levels in Figures 15–17 in each case correspond to the same frequency range (0·576–0·896 Hz). The results indicate that accurate mathematical models of the analyzed

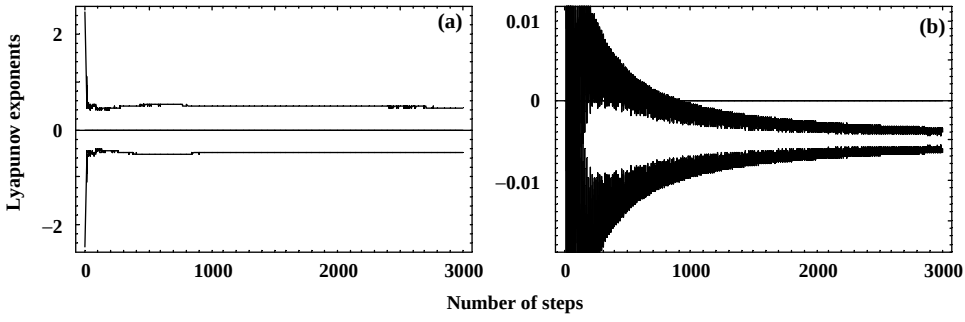

Figure 14. Convergence plot of Lyapunov exponents for system descriptions by (a) equation (9) and (b) equation (10).

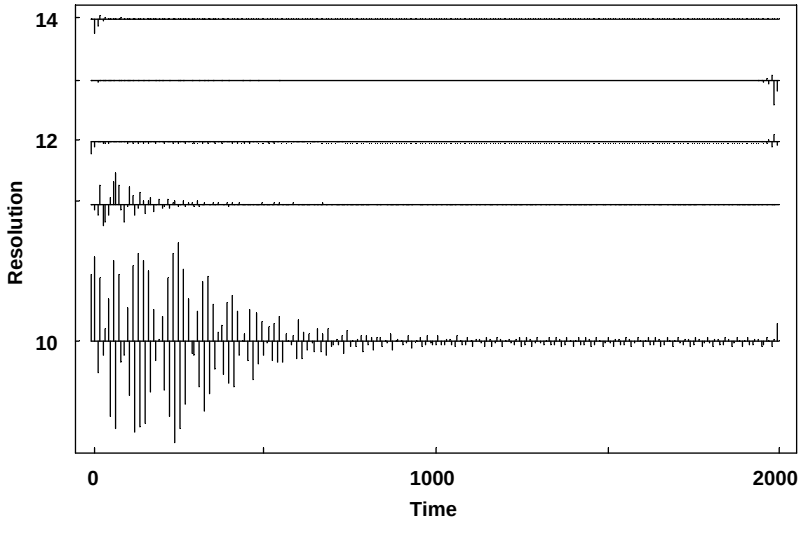

Figure 15. Wavelet coefficients of signal of system described by equation (10).

systems are needed, particularly if such a complex phenomenon as chaos is investigated. Wavelet packet expansion coefficients indicate significant differences between signals but the time traces of the signals are practically indistinguishable. Chaotic solutions have a much larger number of (comparable in absolute value terms) wavelet expansion coefficients and generally the coefficients are distributed over the whole duration of a signal. As previously, the duration of the signal wavelet packet analysis was several times shorter than that of the search for the system's Lyapunov exponents.

5. CONCLUSIONS

A numerical technique, based on discrete signal wavelet analysis, for determining chaotic states of a system has been presented. Using a non-linear 1-d.o.f. system with viscoelastic one-sided constraints as an example, it was shown how a transition from a non-chaotic state to a chaotic state manifests itself in the magnitude and distribution of the system response wavelet expansion coefficients. The classic wavelet analysis algorithm and

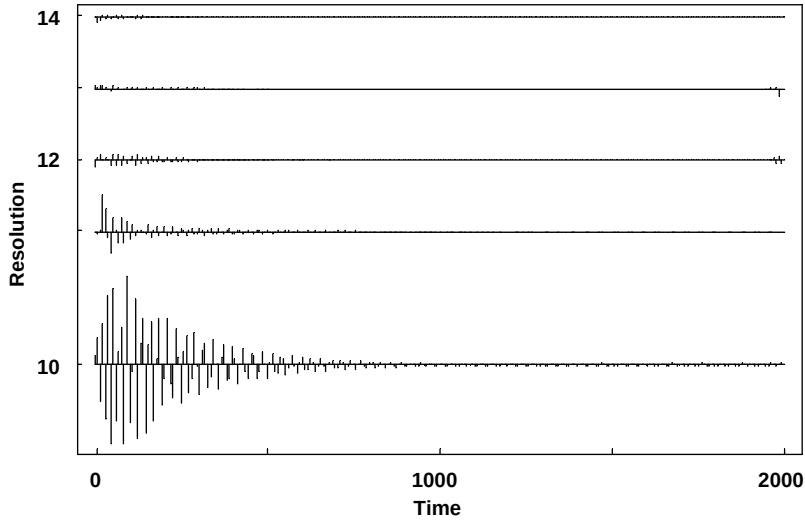

Figure 16. Wavelet coefficients of signal of system described by linearized equation (10) with four terms of expansion $q(t)$ into Taylor series.

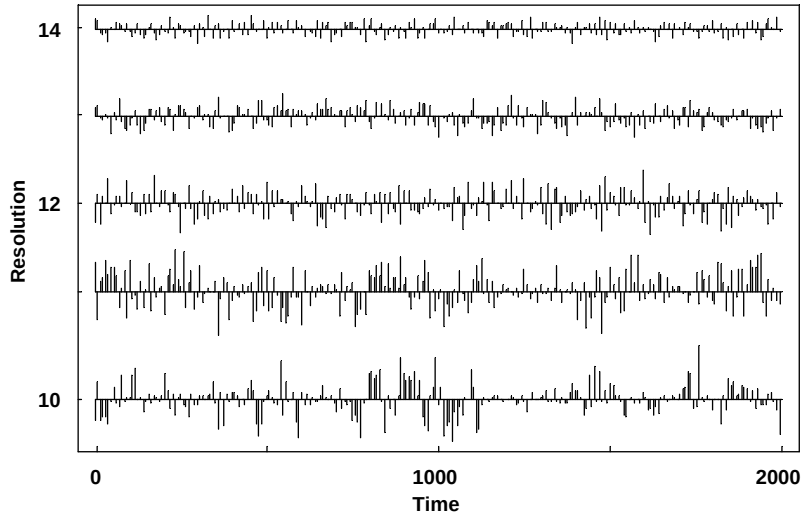

Figure 17. Wavelet coefficients of signal of system described by linearized equation (10) with two terms of expansion $q(t)$ into Taylor series.

packet wavelet analysis were applied. In most cases Daubechies wavelets were used. The conclusions emerging from the wavelet analysis of chaotic and non-chaotic states were verified by an analysis of the system's Lyapunov exponents. On the basis of a series of numerical tests run to determine the system's chaotic states the following conclusions can be drawn:

1. wavelet analysis of a system's response, particularly packet wavelet analysis, may constitute an effective qualitative tool for differentiating between the system's chaotic and non-chaotic states;

2. the duration of a wavelet analysis necessary to differentiate between a system's chaotic and non-chaotic states is at least by two orders shorter than that of a quantitative analysis of the system's Lyapunov exponents;
3. it is possible to differentiate between chaotic and non-chaotic states on the basis of a wavelet analysis of the system's finite, and even short-duration, responses;
4. a characteristic feature of a chaotic signal in wavelet analysis is the usually large number of significant expansion coefficients which generally occur at the low- and high-frequency levels of an analyzed signal;
5. the cumulative energy of a signal may constitute a good tool for identifying its chaotic states—chaotic states are characterized by a large number of comparable (in absolute value terms) expansion coefficients;
6. the best basis location in wavelet packet analysis can serve to distinguish analyzed signals—for chaotic signals, almost exclusively the lowest resolution level is chosen when using minimum entropy criterion;
7. attempts at simplifying mathematical models of systems in which chaos may occur lead, as a rule, to false conclusions about its state and therefore they are inadmissible, as proven conclusively by the wavelet analysis.

Wavelet analysis can be an alternative for different qualitative numerical techniques of identification of chaos, which though similar to these techniques it does not always produce final, equivocal qualification of investigated signals.

REFERENCES

1. T. S. Parker and L. O. Chua 1989 *Practical Numerical Algorithm for Chaotic Systems*. New York: Springer-Verlag.
2. J. Argyris, G. Faust and M. Haase 1994 *An Exploration of Chaos.* Amsterdam: Elsevier Science.
3. G. Chen and X. Dong 1998 *From Chaos to Order. Methodologies, Perspectives and Applications.* Singapore: World Scientific Publishing.
4. Y. Chen and A. Y. T. Leung 1998 *Bifurcation and Chaos in Engineering.* London: Springer-Verlag.
5. C. Robinson 1999 *Dynamical Systems. Stability, Symbolic Dynamics, and Chaos*. Boca Raton, FL: CRC Press.
6. Ch. K. Chui 1992 *An Introduction to Wavelets.* New York: Academic Press.
7. D. E. Newland 1993 *An Introduction to Random Vibrations, Spectral and Wavelet Analysis*. Essex: Longman Group.
8. H. L. Resnikoff and R. O. Wells Jr 1998 *Wavelet Analysis. The Scalable Structure of Information*. New York: Springer-Verlag.
9. J. C. Goswami and A. K. Chan 1999 *Fundamentals of Wavelets. Theory, Algorithms and Application*. New York: John Wiley & Sons.
10. P. Flandrin 1999 *Time–Frequency/Time-Scale Analysis.* San Diego: Academic Press.
11. S. Mallat 1999 *A Wavelet Tour of Signal Processing.* Cambridge: Academic Press.
12. D. E. Newlad 1994 *Journal of Vibration and Acoustics* **116**, 409–416. Wavelet analysis of vibration. Part I: theory.
13. D. E. Newland 1994 *Journal of Vibration and Acoustics* **116**, 417–425. Wavelet analysis of vibration. Part II: wavelet maps.
14. K. Gurley and A. Kareem 1999 *Engineering Structures* **21**, 149–167. Applications of wavelet transforms in earthquake, wind and ocean engineering.
15. Z. Cheng and W. D. Pilkey 1999 *Finite Elements in Analysis and Design* **33**, 233–245. Wavelet-based limiting performance analysis of mechanical systems subject to transient disturbances.
16. B. Basu and V. K. Gupta 1999 *Journal of Sound and Vibration* **222**, 547–563. Wavelet-based analysis of the non-stationary response of a slipping foundation.
17. S. K. Tang 2000 *Journal of Sound and Vibration* **234**, 241–258. On the time–frequency analysis of signals that decay exponentially with time.

18. W. J. Staszewski and G. R. Tomlinson 1994 *Mechanical Systems and Signal Processing* **8**, 289–307. Application of the wavelet transform to fault detection in a spur gear.
19. K. M. Liew and Q. Wang 1998 *Journal of Engineering Mechanics* **124**, 152–157. Application of wavelet theory for crack identification in structures.
20. Q. Wand and X. Deng 1999 *International Journal of Solids and Structures* **36**, 3443–3468. Damage detection with spatial wavelets.
21. J. Lin and L. Qu 2000 *Journal of Sound and Vibration* **234**, 135–148. Feature extraction based on Morlet wavelet and its application for mechanical fault diagnosis.
22. W. J. Staszewski 1998 *Journal of Sound and Vibration* **211**, 735–760. Wavelet based compression and feature selection for vibration analysis.
23. Y. Kitada 1998 *Journal of Engineering Mechanics* **124**, 1059–1066. Identification of nonlinear structural dynamic systems using wavelets.
24. A. N. Robertson, K. C. Park and K. F. Alvin 1998 *Journal of Vibration and Acoustics* **120**, 261–266. Identification of structural dynamics models using wavelet-generated impulse response data.
25. W. J. Staszewski 1997 *Journal of Sound and Vibration* **203**, 283–305. Identification of damping in MDOF systems using time-scale decomposition.
26. M. Ruzzene, A. Fasana, L. Garibaldi and B. Piombo 1997 *Mechanical Systems and Signal Processing* **11**, 207–218. Natural frequencies and dampings identification using wavelet transform: application to real data.
27. C.-H. Lamarque, S. Pernot and A. Cuer 2000 *Journal of Sound and Vibration* **235**, 361–374. Damping identification in multi-degree-of-freedom systems via a wavelet-logarithmic decrement—Part 1: theory.
28. S. Hans, E. Ibraim, S. Pernot, C. Boutin and C.-H. Lamarque 2000 *Journal of Sound and Vibration* **235**, 375–403. Damping identification in multi-degree-of-freedom systems via a wavelet-logarithmic decrement — Part 1: study of a civil engineering building.
29. D. Permann and I. Hamilton 1992 *Physical Review Letters* **69**, 2607–2610. Wavelet analysis of time series for the Duffing oscillator: the detection of order within chaos.
30. W. J. Staszewski and K. Worden 1996 *Proceedings of the International Conference on Nonlinearity, Bifurcation and Chaos, Lodz, Poland*, 222–226. The analysis of chaotic behaviour using fractal and wavelet theory.
31. Z. Jibing, G. Hangshan and G. Yinchao 1998 *Applied Mathematics and Mechanics* **19**, 593–599. Application of wavelet transform to bifurcation and chaos study.
32. F. Mastroddi and A. Bettoli 1999 *Journal of Sound and Vibration* **225**, 887–913. Wavelet analysis for Hopf bifurcations with aeroelastic applications.
33. A. Kyprianou and W. J. Staszewski 1999 *Journal of Sound and Vibration* **228**, 199–210. On the cross wavelet analysis of Duffing oscillator.
34. G. Benettin, L. Galgani, A. Giorgilli and J. M. Strelcyn 1980 *Meccanica* **15**, 21–30. Lyapunov characteristic exponents for smooth dynamical systems and for Hamiltonian systems: a method for computing all of them. Part 2: numerical application.
35. J. P. Eckmann and D. Ruelle 1985 *Reviews of Modern Physics* **57**, 617–656. Ergodic theory of chaos and strange attractors.
36. K. Geist, U. Parlitz and W. Lauterborn 1990 *Progress of Theoretical Physics* **83**, 875–893. Comparison of different methods for computing Lyapunov exponents.
37. G. Cederbaum and M. Mond 1994 *Journal of Sound and Vibration* **176**, 475–486. Instability and chaos in the elastica type problem of parametrically excited columns.
38. R. Van Dooren 1996 *Chaos, Solitons and Fractals* **7**, 77–90. Chaos in a pendulum with forced horizontal support motion: a tutorial.
39. R. Coifman and M. V. Wickerhauser 1992 *IEEE Transactions on Information Theory* **38**, 713–718. Entropy-based algorithms for best basis selection.